AADE-08-DF-HO-10

Agglomeration and Accretion of Drill Cuttings in Water-Based Fluids

S. Cliffe, M-I SWACO and S. Young, M-I SWACO

Abstract

Water-based drilling fluids have evolved as new chemical solutions have been developed to reduce or significantly retard their interaction with claystones and shales. Issues related to cuttings agglomeration and accretion can lead to increased non-productive time which can make water-based drilling fluids less attractive as alternatives to oil-based drilling fluids.

Cuttings agglomeration and accretion are highly dependant on the morphology of the sedimentary rock formations being drilled. Experimental results are presented herein on a number of outcrop shales to show the effect that cuttings type and morphology has on agglomeration. Possible mechanisms for agglomeration, linked to the kinetic hydration and plastic deformation, of cuttings when exposed to water-based drilling fluids are discussed.

High-performance water-based drilling fluids typically contain specific additives to enhance their lubricity and shale inhibitive properties. Adsorption of certain polymers can lead to an increase in the surface stickiness of cuttings and therefore an increased agglomeration potential. Experimental results from testing various encapsulating polymer chemistries are presented, showing that polymers with more hydrophobic moieties are beneficial.

Experimental results will also be presented showing the benefits of certain film-forming additives to reduce the onset of cuttings agglomeration and the negative effects that can occur with certain lubricants based on vegetable oils and fatty acid derivatives. The authors show that careful selection of drilling fluid components can help to reduce the potential for cuttings agglomeration and thus enhance the performance of water-based drilling fluids.

Introduction

The use of high-performance water-based drilling fluids or "muds" (HPWBM) is becoming more widespread as many operators seek alternative, environmentally acceptable, drilling fluid solutions for technically demanding drilling operations. Provided that all of the HPWBM components satisfy local environmental regulations, in most operational areas there are no limitations on the amount of HPWBM which can be discharged.

With the use of oil-based or synthetic-based drilling fluids (OBM/SBM), there is often an associated cost for cuttings remediation, waste-stream processing and compliance testing, all of which must be considered in the economics of the wellbore construction process. The higher operational costs associated with the use of OBM/SBM can sometimes be offset by higher rates of penetration (ROP) and fewer operational problems as compared with conventional water-based drilling fluids (WBM). With the introduction of new chemistry which has been deployed in the new generation of HPWBM, wellbore instability problems have been significantly reduced. However, problems associated with bit balling, agglomeration and accretion of drilled cuttings may still occur, all of which may have the potential to lead to increased non-productive time (NPT) during the drilling process. This can severely detract from the overall performance of the HPWBM.

The phenomena of accretion and agglomeration are still poorly understood, due to a lack of field data, variable drilling practices and changes in formation lithology. In this paper the mechanical deformation of a number of clays is studied to see if a link can be established between either the clay mineral composition or clay plasticity, and the onset of the accretion process.

From close examination of changes in drilling fluid chemistry, exposure time, and applied mechanical load, it was also hoped to make reasonable recommendations on measures which could be applied to minimize cuttings accretion and agglomeration problems during the drilling operation. If the potential for cuttings accretion and agglomeration problems could be mitigated by implementation of simple chemical solutions, the economics of using HPWBM would be further improved by reducing the risk of drilling-fluids-related NPT occurring.

Background

Accretion and Review of Proposed Mechanisms

The first instances of cuttings accretion and accretion-related problems were seen to coincide with the introduction of more inhibitive WBM, typically containing high concentrations of organic molecules such as polyglycerols/ polysaccharides and poly-anionic species (*e.g.* polyphosphates and silicates). The latter are thought to form a barrier at the shale surface to reduce water migration into shales. Early theories based on clay plasticity were proposed to explain the accretion phenomenon.[1,2] These theories are based on the concept of a reduced water penetration into drilled cuttings, slowing down the rate of hydration so that the cuttings remain

in a plastic state over a longer period of time. The extended plasticity state of the clay is thought to allow cuttings to become molded onto the BHA components and plastered onto the near-wellbore wall.

With a less inhibitive mud, such as a potassium chloride/ polymer fluid, these cuttings would normally hydrate more quickly and tend to be less sticky as they continue to adsorb water, resulting in the loss of cohesion in the clay matrix which is more easily removed. However, a lower level of chemical inhibition in WBM can often cause bit balling and wellbore instability problems.

The conditions which should be met for clay agglomeration or accretion to occur are suggested as follows:

(a) The clay is in a plastic state at the equilibrium moisture content when in contact with the drilling fluid. The plastic behavior allows the clay structure to be easily deformed.

(b) The surface of the clay particle is sticky enough to form a bond to other surfaces with which it makes contact.

(c) The surfaces of cuttings must be pushed together (sheared) with sufficient force to deform the clay and create a bond. The effect of mechanical deformation on the phase behavior of clay particles is a consideration which has been overlooked in the past.

The current range of HPWBM contains additives to prevent transfer of water to the formation and reduce clay hydration. The vast majority of shales and claystones drilled contain expandable clay minerals which will have a strong tendency to swell when exposed to a continuous phase containing water. Low-molecular-weight amines, polyamines and polyether-amines are some examples of the chemistries that can be used to reduce interstitial clay swelling.

An encapsulating polymer is also often used in conjunction with such primary shale swelling inhibitors. The encapsulating polymer adsorbs onto drilled cuttings and onto the near-wellbore wall to minimize dispersion and wellbore erosion.

In addition, increasingly, additives are being recommended to reduce the potential for bit balling, cutting agglomeration and accretion problems. There seems to be a consensus in the industry that these additives function by coating steel and cuttings surfaces to form a hydrophobic film which reduces the adhesion of hydrated clays to the BHA and also helps to prevent cuttings agglomeration.[3,4,5,6,7,8,9]

Other innovative approaches to prevent bit balling are described in the literature that involve applying a low-friction polymer coating to the bit[10] or from applying a negative potential which generates an electro-osmotic effect.[11] Although engineering solutions to bit balling and accretion are very interesting, they are outside the scope of this paper.

Clay Structure and Reactivity

The clay minerals which are commonly found in shales and claystones can broadly be grouped into kaolinite, smectite, mica, and chlorite. The crystalline structures of these clay minerals and mixed layer structures are described extensively in the literature.[12] In simple terms, clays can be categorized depending on the way that tetrahedral and octahedral sheets are packaged into layers and on the composition of the tetrahedral and octahedral sheets. Changes in the composition of the layers results in the layers having a net negative charge.

Clay behavior is largely dependent on the interaction between the basic structural framework and the pore fluid, with the interactions being mainly chemical or electro-chemical in nature. This is believed to arise from the unsatisfied electrical charge of clay platelets, which affects the structure and behavior of water in the vicinity of the clay platelet. The residual repulsion between clay platelets, due to hydration of the clay surfaces and sterical interferences between hydrated ions and water molecules, gives rise to a net swelling pressure,[2] which will vary greatly between differing clay minerals. The type and concentrations of clay minerals present will determine how chemical inhibitors affect the swelling response of bulk clays on contact with water.

Atterberg Limits

The Atterberg limits of a soil or clay are the liquid limit (LL), plastic limit (PL), and plastic index and are fully defined in the published literature.[13] Various researchers have attempted to correlate the Atterberg limits with clay mineral composition, cation exchange capacity and swelling characteristics.

The ***liquid limit*** is the moisture content, expressed as a percentage by weight of the oven-dry soil, at which the soil will just begin to flow when jarred slightly.

The ***plastic limit*** is the lowest moisture content, expressed as a percentage by weight of the oven-dry soil, at which the soil can be rolled into ⅛-in. diameter threads without breaking into pieces. Soil which cannot be rolled into threads at any moisture content is considered non-plastic.

The ***plastic index*** is the difference between the liquid limit and the plastic limit. It is the range of moisture content through which a soil is plastic. When the plastic limit is equal to or greater than the liquid limit, the plastic index is recorded as zero.

White[14] determined the Atterberg Limits of four homoionic montmorillonites and concluded that the structure of the clay minerals seems to be the most important factor in determining the properties of clay-water systems. The cation exerts a secondary influence by which it can only act to alter the properties established by the structure of the clay mineral. Structure is probably determined by the location of the substitutions within the lattice and by the distribution of the substitutions.

Extensive studies on montmorillonitic and kaolinitic soils have been carried out by Sridharan et al.[15,16,17] who concluded that diffuse double-layer repulsion has a dominant influence for montmorillonitic clay, with the liquid limit increasing with the increasing hydrated radius of the adsorbed cation,. For kaolinitic clays the electrical attractive forces and particle orientation in the fabric play a prominent role. Kaolinite soils with a greater degree of flocculation will have larger void spaces and exhibit higher liquid-limit values, whereas soils with a lesser degree of particle flocculation will have

relatively smaller void spaces, and consequently, exhibit lower liquid-limit values. This means that the mechanisms controlling clay behavior can be entirely different depending on whether the primary mineral is kaolinite or montmorillonite. It follows that the chemical effects of drilling fluid additives should be carefully selected if the mechanical properties of clays are to be better controlled.

In more recent work Sridharan et al. concluded that both liquid limit and plastic limit are primarily a function of percent clay fraction, clay mineral type and the type of associated cations present.[18] The results of this work are summarized in Tables 1 and 2. The ratio of PL/LL was seen to increase in the following series:

Na-bentonite < *Illite* < *Kaolinite* < *Halloysite*

A relationship was also proposed which could be used to classify soils as kaolinitic or montmorillonitic by examining the PL/LL ratio. Clays with a higher montmorillonite fraction and lower kaolinite fraction tend to have a lower PL/LL ratio.

A correlation between the valency and size of the adsorbed cation and the index properties of bentonite clays was seen. The PL/LL ratio was also seen to increase with increasing valency and as hydrated ionic radius increases, according to the series below.

$Na^{+} < K^{+} < Ca^{2+} < Mg^{2+} < Fe^{3+} < Al^{3+}$

In addition, when sand or silt is introduced as a diluent, a reduction in the magnitude of the plastic and liquid limits values was observed, but the PL/LL ratio was seen to remain constant.

These concepts described above, coupled with X-ray powder diffraction (XRPD) studies and determination of Atterberg limits, are used later on in this paper to propose an explanation of the experimental results obtained at the macroscopic scale.

Characterization of Outcrop Clay Samples

Description

Preserved outcrop shale samples were used in the experimental work described in this paper. The clays were kept in a controlled environment to preserve the water content as closely to the natural state as possible. The clays selected for the study have a broad range of reactivity from highly dispersive (Arne clay) to moderate/highly swelling (Oxford/Green-Lillebaelt clays).

Oxford Clay is a swelling and moderately dispersive shale of Jurassic origin.

London Clay is a plastic, swelling and very dispersible Tertiary clay.

Foss Eikeland clay is a dispersive clay from an outcrop in Norway.

Arne Clay is described as a ball clay with high kaolinite content and is extremely dispersive in contact with water.

Green-(Lillebael)t Clay is fine-grained swelling clay from an outcrop in Denmark.

London, Oxford and Arne clays are all sourced from outcrops in southern England.

Cation Exchange Capacity (CEC)

The CEC of each outcrop shale was determined by the standard API Methylene Blue titration method. Results are given in Table 3.

X-ray Powder Diffraction (XRPD) Analysis

The outcrop clays described above were submitted for analysis by X-ray powder diffraction.

The bulk sample was wet ground and spray dried to produce a random powder to which 20 wt% Corundum (crystalline aluminum oxide) was added to act as an internal standard for quantitative phase analysis (QPA). XRPD patterns were recorded from 2–75°2θ using Cobalt Kα radiation. QPA was conducted by a reference intensity ratio (RIR) method.

Clay fractions of less than 2 μm were obtained by timed sedimentation, prepared as oriented mounts using the filter peel transfer technique and scanned from 2–45°2θ in the air-dried state, after glycolation, and after heating to 300°C for one hour. Clay minerals identified were quantified using a mineral intensity factor approach based on calculated XRPD patterns. The XRPD patterns, with the main phases identified by reference to patterns from the International Centre for Diffraction Database (ICDD), are provided for reference.

The outcrop clay samples vary in mineralogy. They are all dominated by dioctahedral clay minerals (illite, illite-smectite and kaolinite) with smaller amounts of quartz, feldspars, carbonates, pyrite, anatase, chlorite and anhydrite. The Lillebaelt clay sample had a higher calcite content than the other samples.

The less than 2-μm clay fractions show a variable mineralogy, dominated by illite-smectite and illite in most cases, with subordinate kaolinite and chlorite. The Arne clay sample contains a significantly higher kaolinite content than the other clay samples. The mixed-layer illite-smectite varies in individual clay samples. The expandability of this material in the London clay and Green(Lillebaelt) clay is high (80 – 90%) but moderate to low in the other three clays (30 – 50%).

A complete mineral breakdown is summarized in Tables 4 and 5.

Plastic and Liquid Limits

Each clay sample was allowed to air dry for a period of 72 hr and was then ground to a fine powder. The residue remaining on a 425-μm sieve was discarded. The clay powder fraction of less than 425 micron was used to determine plastic and liquid limits, according to the standard method (ASTM D4318).

Liquid limits were measured using the Casagrande apparatus[13]. The number of drops (revolutions) which was required for a groove cut in the clay paste to close by a length of 13 mm was measured. After each test, and further addition of water, a small amount of sample was dried to constant weight and the percent water content calculated based on the dry weight of the sample. A plot of the number of drops (x-axis) versus water content (y-axis) was then constructed. The

LL (y-axis) was taken from the straight-line plot corresponding to 25 drops (x-axis).

Plastic limits were determined by adding water to the clay sample, shaping it into an ellipsoidal mass and rolling it into a thread between the fingers and a glass plate. The PL was considered to have been reached at the point at which a 3-mm thread could be rolled out without crumbling or sticking to the glass plate. The recovered threads were then dried to constant weight. The PL is calculated as the percent water content of the clay threads based on dry weight of the sample.

LL and PL results are summarized in Table 6.

The native water contents were also measured, expressed as percentage by weight water, based on the wet state. Results are summarized in Table 7.

Accretion Study

Rolling Bar Test Method

The mild steel bar, used in each test, was first cleaned to remove surface rust and any chemical deposits from previous tests. The bar was subjected to a rigorous cleaning cycle that included a detergent wash, treatment with 200-grit wet abrasive paper and rinsing with clean water. The surface of the bar was then dried and given a further cleaning with acetone to remove any residual deposits of oil/grease. Each bar was placed centrally in the test cell, and the cell was half filled with test fluid. The generic formulation of the 12.5-lbm/gal HPWBM test fluid used is given in Table 8.

A 50-g sample of sized cuttings with a narrow particle-size distribution was added to each and evenly distributed around the central bar. Gentle agitation was then applied with a spatula to ensure an even distribution of the solids in the fluid. The cell was then topped up with additional test fluid to the rim of the cell and sealed. The cell was inverted 3–4 times to minimize the chances of cuttings sticking to the bottom of the cell; the cell was then transferred to a rolling oven.

After rolling the cell for a defined time interval (t) at room temperature, the bar was removed and quickly washed with a gentle stream of tap water. The bar was then rolled on an adsorbent paper towel to remove excess surface fluid. The accreted solids were then scraped off, weighed (w1), dried to constant weight at 105°C and then reweighed (w2).

Accretion is calculated from the weight of clay solids adhering after time (t), expressed as a % of the dry clay fraction (corrected from the initial, native, water content of the unexposed cuttings sample, M_i).

$$\%A = \frac{w2}{[(100-M_i)/100]\ x50} \qquad \text{(Eq. 1)}$$

The moisture content (%M) of any agglomerated solids is also measured to determine the degree of hydration of the agglomerated material.

$$\%M = \frac{w2 - w1}{w1}\ x100 \qquad \text{(Eq. 2)}$$

To determine the rate of cuttings agglomeration and accretion onto the steel bar, accretion tests were run at increasing time intervals, with a separate test for each time interval.

The standard accretion test used throughout the experimental study described in this paper was based on a solid steel bar (SSB) of dimensions: 150-mm length, 23.7-mm diameter and 527-g weight. The diameter of the cell used was 63 mm. A picture of the SSB and cell configuration is shown in Figure 1. An alternative methodology, using a hollow steel tube (HST), was used to determine the effect of reduced mechanical load on the kinetics of accretion, the findings of which will be discussed later in the paper. This configuration is shown in Figure 2.

Effect of Shale Type on Accretion

The standard outcrop shale samples were all sized into discrete cuttings, with a particle-size distribution of 4.8 to 6.3 mm. The amount of clay solids adhering to a SSB (in the standard accretion method) was measured at increasing time intervals. The water contents of the accreted solids were also measured. Figures 3 to 7 show the appearance and magnitude of accreted material, and show that cuttings first undergo a deformation process before forming a more uniform accreted layer. The time dependence of the accretion process can be seen from the data presented as Figure 8, with accretion maxima occurring between 20 – 30 min. It is particularly noticeable that Arne clay had a much broader accretion profile than the other outcrop shales studied, and that there is much greater scatter in the data.

The initial rates of solids buildup can be better seen from the data presented as Figure 9. Green (Lillebaelt) and Oxford clays appear to need a longer initiation time for the deformation and accretion process to occur.

The data presented in Figure 10 shows the relationship between percent water content of accreted solids and exposure time. There appears to be a very rapid uptake of water by the outcrop shale cuttings after a short exposure time (5 – 10 min). Cuttings still continue to hydrate with increasing exposure time, albeit at a slower rate. The data presented in both Figures 10 and 11 shows a wide variation in the hydration state of accreted solids, and this was seen to be very dependent on the outcrop clay type. Figure 11 shows percent water contents for accreted solids, where %A is greater than 50%, and may also suggest that the width of the hydration envelope is indicative of the time scale where there is a probability of accretion.

Effect of Shale Composition on Accretion

The kaolinite, illite and illite-smectite mineral contents present in the bulk shale sample can be calculated, based on the assumption that the <2-μm clay fraction is representative of the bulk clay fraction. These calculated clay fractions are summarized in Table 9. Accretion figures and associated water contents are also summarized in Tables 10 and 11 at selected time intervals.

If the water content of accreted solids recovered after specific exposure times are plotted against the calculated bulk percent mineral fractions, a very good correlation is seen in the data with illite and illite-smectite mineral fractions, whereas the correlation with the kaolinite mineral fraction is much weaker (Figures 12–14).

Analysis of the accretion data is more difficult. Generally, there is less of a correlation between accretion and percent mineral fraction at shorter time intervals (5 min). A stronger correlation exists after a 10-min exposure period. With increasing exposure time, the correlation between illite and illite-smectite percent mineral fractions is seen to deteriorate. Conversely, the correlation of accretion with kaolinite percent mineral fraction is seen to markedly improve over a 60-min time frame. This type of behavior might be expected for complex shales which contain component parts of different reactivity (Figures 15 – 17).

Effect of Atterberg Limits on Accretion

Contrary to the findings of Sridharan et al.,[18] a strong trend was not observed between the PL/LL ratio and percent clay mineral fraction or accretion, based on the limited data set available. However, a fair correlation was observed between PL and accretion. A similar correlation was also observed between PL and the water content of accreted solids (Figures 18 – 21).

Effect of Initial Water Content on Accretion

A sample of Oxford clay cuttings with a particle-size distribution of 2.4 – 4.8 mm was allowed to air dry for a period of 72 hr. The amount of clay solids adhering to a SSB (in the standard accretion method) was measured at increasing time intervals, and compared to results from parallel tests conducted on a sample of cuttings of similar size distribution preserved at native moisture content. The initial water content of the dried sample was measured at 2.6% compared to 20.6% in the preserved sample. Accretion and water content for the two clay samples are shown in Figures 22 and 23. The results show a reduced tendency for cuttings to accrete if they have intrinsically lower water content, even though the hydration process of accreted solids is fairly rapid. The accretion curves eventually coalesce, but accreted solids are still significantly less hydrated, arising from the cuttings with lower initial water content.

Effect of Cuttings Size on Accretion

Various sized fractions of Oxford clay cuttings were prepared. The amount of clay solids adhering to a SSB (in the standard accretion method) was measured at increasing time intervals. Results are shown in Figure 24. It can be seen that with increasing cuttings size there is a general reduction in the levels of accretion observed, particularly after shorter exposure times. Looking at the data in a different way (Figure 25), it can be seen that in general an increase in cuttings size reduces the rate of accretion, with the accretion maxima requiring longer times to develop.

The lower level of accretion observed from Oxford clay cuttings with the smallest particle-size distribution, in this case less than 2 mm, is attributed to more rapid disintegration of these cuttings due to their higher surface area. This is another effect that needs to be taken into consideration.

Effect of Mechanical Force on Accretion

The effect of mechanical force on the deformation of cuttings and on the kinetics of accretion was studied by substituting the SSB with a hollow steel tube (HST), of dimensions: 120-mm length, 35-mm diameter, 138-g weight. Accretion profiles are shown in Figures 26 and 27 for both the SSB and HST methods, using 4.7- to 6.3-mm sized Oxford clay and Arne clay cuttings, The onset of accretion appears to be significantly delayed with the lighter HST compared to the SSB, which results in a displacement of the accretion profiles to longer times. In addition, the accretion profiles occur over significantly wider time periods with the HST. In separate cuttings dispersion tests, using identical drilling fluid components to the ones used in this study, there were no visible signs of cuttings agglomeration even with a much longer exposure time and heating (16 hr at 150°F). These results indicate that some mechanical deformation of cuttings must occur before accretion and agglomeration can take place.

Effect of Drilling Fluid Additives

In a supplementary study, the effects of varying chemistry and concentration of specific drilling fluid components on accretion were investigated. This initial investigation has already led to the development of some novel chemical solutions to reduce cuttings accretion and agglomeration. Figures 28 and 29 show the benefits of two new, novel encapsulating polymers (Polymer C and Polymer D) compared to Polymer A. The latter is based on conventional polyacrylamide encapsulator chemistry, which has been widely used in WBM.

The effect of a number of anticrete additives of varying composition and at varying concentrations are shown in Figures 30 and 31. It is apparent from the data presented that the effective concentration of the anticrete must be considered if accretion is to be sufficiently controlled. New anticrete formulations (Anticrete #2) have been developed which form stronger interfacial films on the surfaces of cuttings and are subsequently more effective at lower concentrations.

During the course of the investigation into the composition of anticretes it was observed that certain fatty acid and fatty ester-based lubricants can actually increase cuttings agglomeration and accretion problems. Figure 32 summarizes some of the lubricant investigation data, showing that the addition of certain lubricants can have a detrimental effect on accretion.

Conclusions

Both from investigations into accretion incidents from the field and from the extensive laboratory studies carried out, there is significant evidence to indicate that shales that contain a higher percentage of illite and kaolinite mineral fractions

will be more susceptible to accretion when exposed to HPWBM.

Accreted solids tend to become more hydrated when composed of clays containing higher percentages of illite-smectite mineral fractions. In contrast, lower levels of hydration are observed with higher percentage mineral fractions of illite and kaolinite.

A strong trend was not observed between PL/LL ratio and either percent clay mineral fraction or percent accretion, based on the limited data set gathered in these experiments. However, a good correlation was observed between PL and accretion. A similar correlation was also observed between PL and the water content of accreted solids. From the experimental data it is believed that use of Atterberg limits could be helpful in predicting which shale types have the greatest accretion tendency. This would, however, require reliable samples of substantially unaltered clays.

It was also experimentally shown that the accretion process can be substantially reduced by lowering the native water content of the cuttings or by generating a larger particle-size distribution of cuttings. Greater drilling performance advantages can thus be taken by better matching bit type to both formation type and selection of the HPWBM composition.

Some mechanical degradation of cuttings is necessary for the accretion process to occur, thus taking steps to optimize ROP, and cutting transportation can have benefits in reducing accretion tendency.

The careful selection of drilling fluid components, trying to better match these to the anticipated shale properties, can certainly reduce accretion tendency. Continuing with this type of work and using the results to assist in the design of new encapsulating polymers and anticrete additives will give benefits in reduced accretion potential and improved performance from the HPWBM.

Acknowledgments

XRPD analysis and data interpretation was carried out by Macaulay Analytical Services, Macaulay Enterprises Limited, Aberdeen, UK.

The authors would like to thank M-I SWACO for sponsoring this work and for permission to present this paper.

Nomenclature

HPWBM = High-performance water-based drilling fluid
CEC = Cationic exchange capacity

References

1. Reid, P.I., Minton, R.C., and Twynam, A. "Field Valuation of a Novel Inhibitive Water-Based Drilling Fluid for Tertiary Shales." SPE 24979, European Petroleum Conference, Cannes, France, 16-18 November 1992.
2. van Oort, E. "On the Physical and Chemical Stability of Shales." *Journal of Petroleum Science and Engineering* (2003) v38, 213-235.
3. Growcock, F.B., Sinor, L.A., Reece, A.R., and Powers, J.R., "Innovative Additives Can Increase the Drilling Rates of Water-Based Muds." SPE 28708, SPE International Petroleum Conference and Exhibition of Mexico, Veracruz, Mexico, 10-13 October 1994.
4. van Oort, E., Bland, R., Pessier, R., and Christensen, H. "Drilling More Stable Wells Faster and Cheaper with PDC Bits and Water Based Muds." SPE 59192, SPE/IADC Drilling Conference, New Orleans, 23-25 February 2000.
5. Morton, K., Bomar, B., Schiller, M., Gallet, J., Azar, S., Dye, W., Daugereau, K., Hansen, N., Otto, M., Leaper, R., and Shoults, L. "Selection and Evaluation Criteria for High-Performance Drilling Fluids." SPE 96342, SPE Annual Technical Conference, Dallas, 9-12 October 2005.
6. Klein, A.L., Aldea, C., Bruton, J.R., and Dobbs, W.R. "Field Verification: Invert Mud Performance from Water-Based Mud in Gulf of Mexico Shelf." SPE 84314, SPE Annual Technical Conference, Denver, Colorado, 5-8 October 2003.
7. Dye, W., Daugereau, K., Hansen, N., Otto, M., Shoults, L., Leaper, R., Clapper, D., and Xiang, T. "New Water-Based Mud Balances High-Performance Drilling and Environmental Compliance." SPE 92367, SPE/IADC Drilling Conference, Amsterdam, 23-25 February 2005.
8. Al-Ansari, A., Yadav, K., Anderson, D., Leaper, R., Dye, W., and Hansen, N. "Diverse Application of Unique High Performance Water Based Mud Technology in the Middle East." SPE 97314, SPE/IADC Middle East Drilling Technology Conference, Dubai, 12-14 September 2005.
9. Montilva, J., van Oort, E., Brahim, R., Luzardo,J.P., McDonald, M., Quintero, L., Dye, W. and Trenery, J., "Using a Low-Salinity High-Performance Water-Based Drilling Fluid for Improved Drilling Performance in Lake Maracaibo." SPE 110366, SPE Annual Technical Conference, Anaheim, California, 11-14 November 2007.
10. Mat, M.R., Bin Zakaria, M.Z., Radford, S., Eckstrom, D., and Christensen, H. "Innovative Low-Friction Coating Reduces PDC Balling and Doubles ROP Drilling Shales with WBM." SPE 74514, SPE/IADC Drilling Conference, Dallas, 26-28 February 2002.
11. Cooper, G.A. and Roy, S. "Prevention of Bit Balling by Electro-Osmosis." SPE 27882, SPE Western Regional Meeting, Long Beach, California, 23-25 March 1994.
12. Grim, R.E. *Clay Mineralogy*. McGraw-Hill (1968) 51-122.
13. Allen, H. "Classification of Soils and Control Procedures Used in Construction of Embankments." *Public Roads* (1942) v22, 263-265.
14. White, W.A. "Water Sorption Properties of Homoionic Montmorillonite." *Clays and Clay Minerals*. (1954) v3, #1, 186-204.
15. Sridharan, A. and Rao, G.V. "Mechanisms Controlling the Liquid Limit of Clays." *Proc. Istanbul Conf. on Soil Mech. and Found Eng.* (1975) v1, 65-74.
16. Sridharan, A., Rao, S.M., and Murthy, N.S. "Liquid Limit of Montmorilonite Soils." *Geotechnical Testing J*. (1986) v9,#3, 156-159.
17. Sridharan, A., Rao, S.M., and Murthy, N.S. "Liquid Limit of Kaolinite Soils." *Geotechnique* (1988) v38,#2, 191-198.
18. Sridharan, A., Rao, P.R. and Miura, N. "Characterisation of Ariake and other Marine Clays." *Proceedings of International Symposium on Lowland Technology* (2004) 53-58.

Table 1 – PL/LL Ratios for Various Clay Minerals
(Sridharan et al.[18])

Clay Mineral	Ratio of PL/LL
Na-Bentonite	0.07 – 0.26
Illite	0.31 – 0.51
Kaolinite	0.36 – 0.70
Attapulgite	0.54
Halloysite	0.88

Table 2 – Influence of Valency and Size of Adsorbed Cations on the Index Properties of Bentonites (Sridharan et al.[18])

Bentonite-homoionized	PL	LL	Ratio of PL/LL
Li^{+}, Lithium	49.1	675	0.073
Na^{+}, Sodium	19.2	495	0.099
NH^{4+}, Ammonium	55.8	223	0.250
K^{+}, Potassium	57.8	233	0.248
Ca^{2+}, Calcium	40.6	125	0.325
Mg^{2+}, Magnesium	49.9	129	0.387
Ba^{2+}, Barium	45.8	108	0.424
Al^{3+}, Aluminium	60.5	108	0.560
Fe^{3+}, Iron	63.5	120	0.524

Table 3 – CEC of Outcrop Clays

Sample ID	CEC (meq/100 g)
Arne Clay	7 - 16
Foss Eikeland Clay	14
London Clay	20
Green Clay(Lillebaelt)	41
Oxford Clay	22

Table 4 – XRPD Analysis on Bulk Clay Fraction

Sample ID	Quartz	Plagioclase	K-fspar	Calcite	Dolomite	Siderite
Arne Clay	14.8	1.4	1.5	0.9	0	0.3
Foss Eikeland Clay	22.1	18.1	11.2	2.6	1	0.5
London Clay	24.4	1.9	4.3	1.4	1.6	0.7
Green Clay (Lillebaelt)	3.6	1.2	2.6	21.8	0	0
Oxford Clay	18.9	1.5	3	8	0.5	1

Sample ID	Pyrite	Anatase	Anhydrite	Kaolinite	Dioctahedral Clays	Trioctahedral Clays
Arne Clay	0	0.47	0.77	33.86	44.49	0
Foss Eikeland Clay	1.4	0	0	1.38	35.4	5
London Clay	1.2	0.19	0.8	8.96	47.3	3.8
Green Clay (Lillebaelt)	0	0	0	8	67.6	0
Oxford Clay	2.9	0.4	0.3	12.8	47.3	3.8

Table 5 – Relative Percentage of Clay Minerals in the <2-mm Clay Size Fraction

Sample ID	Chlorite	Kaolinite	Illite	Illite-Smectite
Arne Clay	1	35	36	28
Foss Eikeland Clay	3	10	41	47
London Clay	1	9	17	74
Green Clay (Lillebaelt)	1	5	3	91
Oxford Clay	2	8	19	72

Table 6 – Atterberg Limits Measured on Outcrop Clays

Sample ID	PL	LL	PI	Ratio of PL/LL
Arne Clay	34.6	69.4	34.8	0.50
Foss Eikeland Clay	30.1	81.2	51.1	0.37
London Clay	34.6	70.8	36.2	0.49
Green Clay (Lillebaelt)	56.9	273	216.1	0.21
Oxford Clay	36.1	70.9	34.8	0.51

Table 7 – Percentage Water Content of Outcrop Clays (Native State and at the Atterberg Limit Values)

Sample ID	% water at native state	% water at plastic state	% water at liquid state
Arne Clay	3.4	25.7	40.9
Foss Eikeland Clay	17.0	23.1	44.7
London Clay	20.5	25.7	41.4
Green Clay (Lillebaelt)	26.5	36.3	73.2
Oxford Clay	20.5	26.5	41.5

Table 8 – Generic HPWBM formulation

Table 8 – Generic HPWBM Formulation

Product	Concentration (g)
Freshwater	265.1
KCl	14
NaCl	14
Shale hydration inhibitor	10.8
Xanthan gum	0.7
Polyanionic Cellulose LV	1.1
Modified starch	3.2
Encapsulating polymer	2.1
Barite	214.1

Table 9 - Relative Percent Clay Fraction in Bulk Sample

Sample ID	Arne Clay	Foss Eikeland Clay	London Clay	Green Clay (Lillebaelt)	Oxford Clay
Kaolinite	33.9	1.4	9.0	8.0	12.8
Illite	24.6	18.2	9.4	2.1	10.4
Illite-Smectite	19.2	20.9	41.1	64.8	39.6

Table 10 – Percentage Water Content of Accreted Solids vs. Time (SSB Test Method)

Time (min)	% H_2O				
	Arne Clay	Foss Eikeland Clay	London Clay	Green Clay-Lillebaelt	Oxford clay
5	25.4	25.8	30.7	35	31.1
10	26.3	27.4	32.8	36.8	31.3
30	27.2	28.2	33.5	37.6	33.2
60	27.6	29.4	34.5	37.7	35.1

Table 11 – Percentage Accreted Solids vs. Time (SSB Test Method)

Time (min)	% Accretion				
	Arne Clay	Foss Eikeland Clay	London Clay	Green Clay-Lillebaelt	Oxford Clay
5	73.4	76.2	75.1	20.3	47.2
10	110.3	101.8	89.1	72.7	92
30	111.1	101.6	74.2	87.3	95.8
60	109.4	2.0	51.5	38.4	50.2

Figure 1 – Accretion Test Cell – Solid Steel Bar (SSB).

Figure 2 – Accretion Test Cell-Hollow Steel Tube (HST)

Figure 3 – Accretion profiles for Arne Clay (5-, 10-, 20-, 40-, 60-, and 80-min time intervals).

Figure 4 – Accretion profiles for Foss Eikeland Clay (5-, 10-, 20-, 40-, and 60-min time intervals).

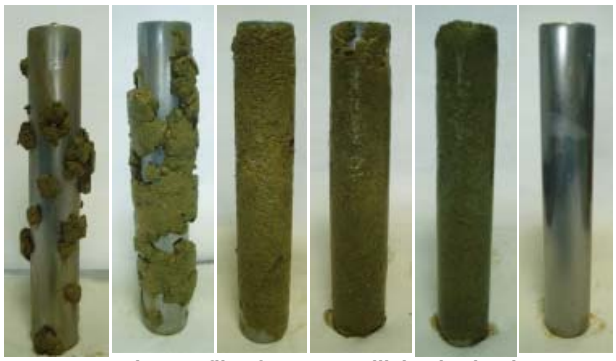

Figure 5 – Accretion profiles for Green-Lillebaelt Clay (5-, 10-, 20-, 40-, 60-, and 80-min time intervals).

Figure 6 – Accretion profiles for London Clay (5-, 10-, 20-, 40-, 60-, and 80-min time intervals).

Figure 7 – Accretion profiles for Oxford Clay (5, 10, 20, 40, 60 and 80 minute time intervals).

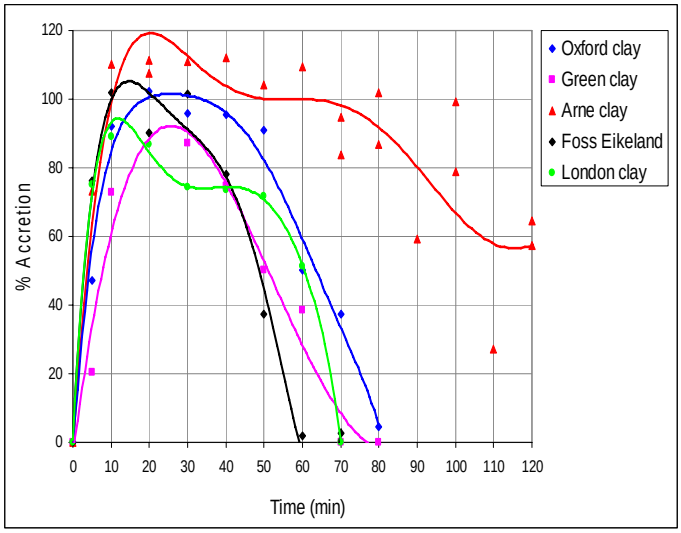

Figure 8 – Effect of shale type on accretion-time profiles.

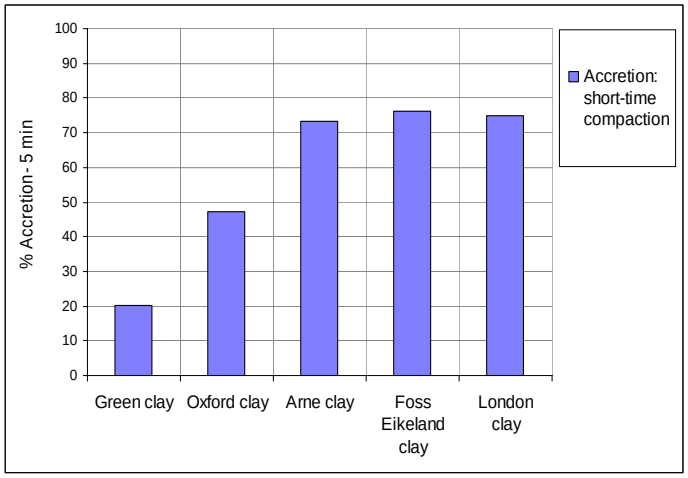

Figure 9 – Effect of shale type on the initial onset of accretion.

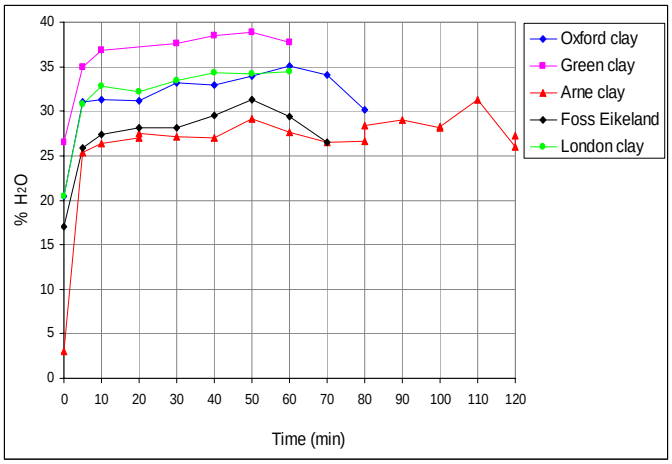

Figure 10 – Variation in the percent water content of accreted solids vs. time.

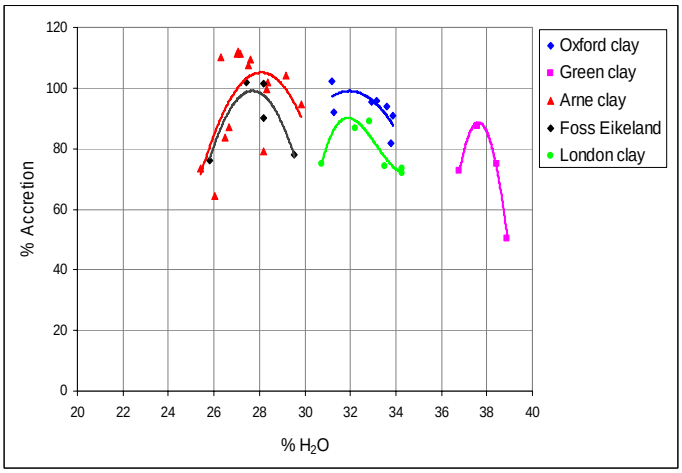

Figure 11 – Hydration curves for accreted solids, where %A > 50%.

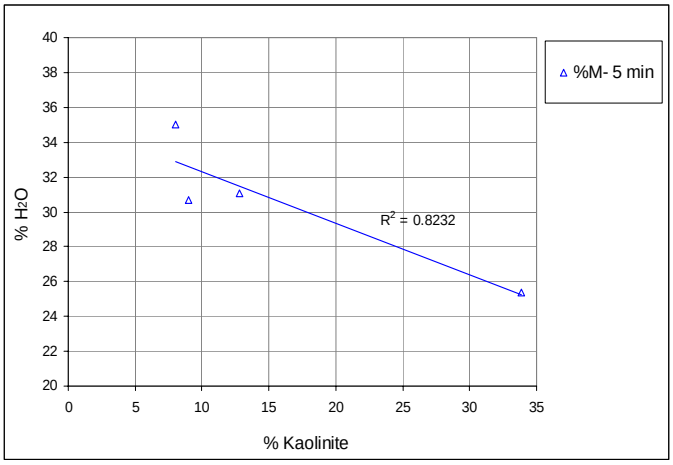

Figure 12 – Effect of percent kaolinite fraction on water content of accreted solids.

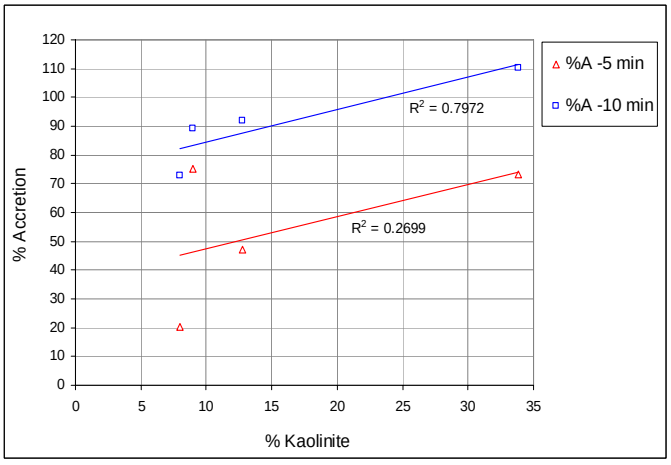

Figure 15 – Effect of percent kaolinite fraction on accretion (t=5, 10 min).

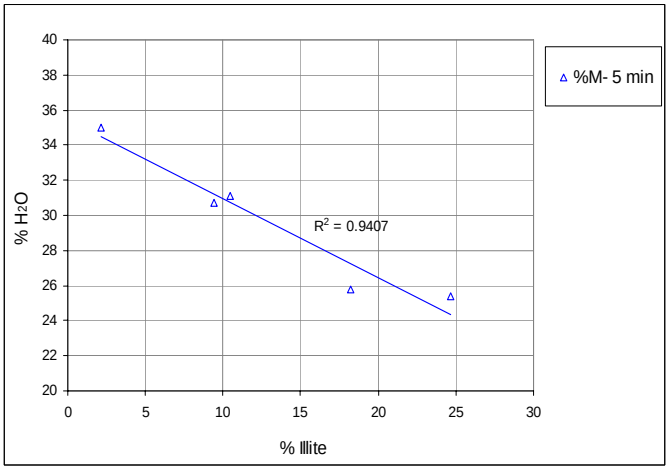

Figure 13 – Effect of percent illite fraction on water content of accreted solids.

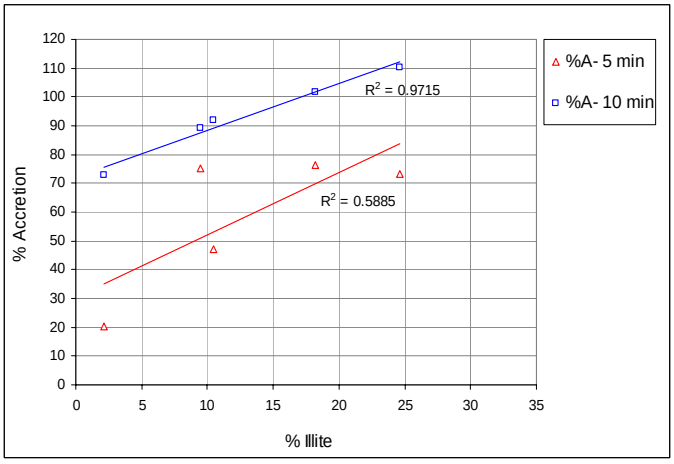

Figure 16 – Effect of percent illite fraction on accretion (t=5, 10 min).

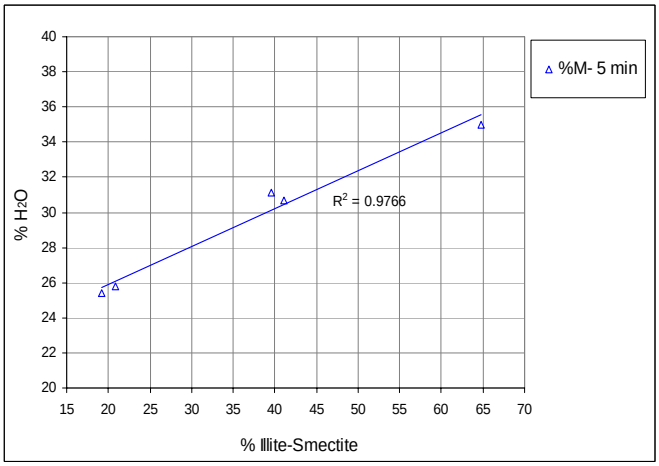

Figure 14 – Effect of percent illite-smectite fraction on water content of accreted solids.

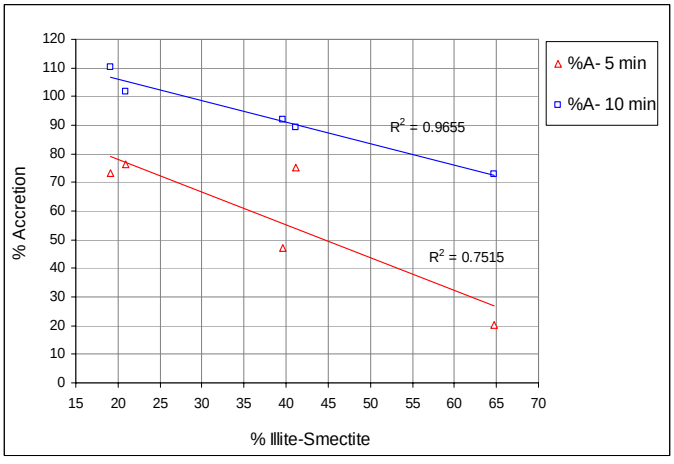

Figure 17 – Effect of percent illite-smectite fraction on accretion (t=5, 10 min).

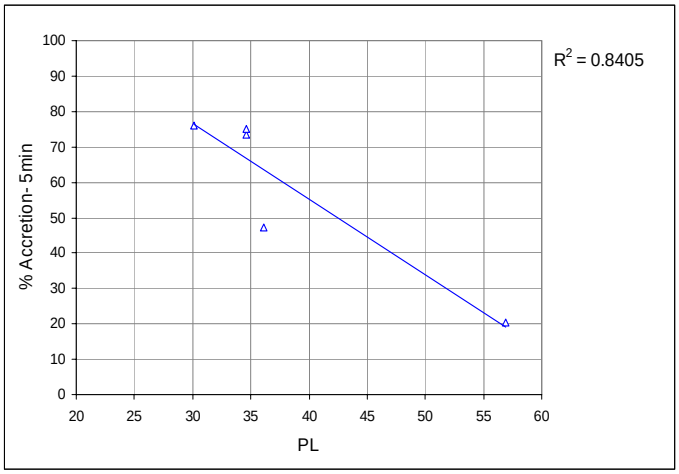

Figure 18 – Effect of PL on accretion (t=5 min).

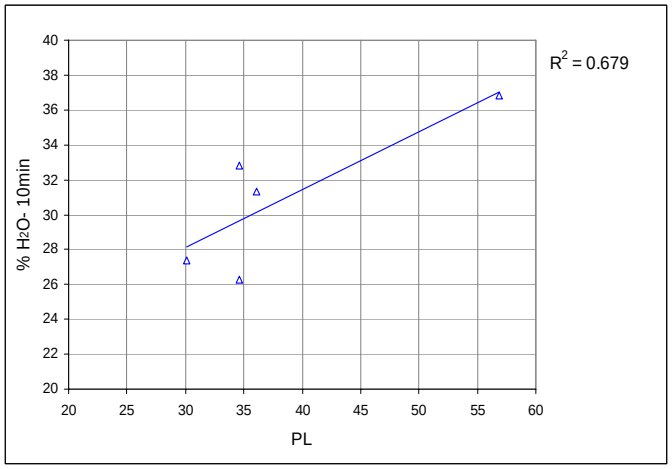

Figure 21 – Effect of PL on percent water content of accreted solids (t=10 min).

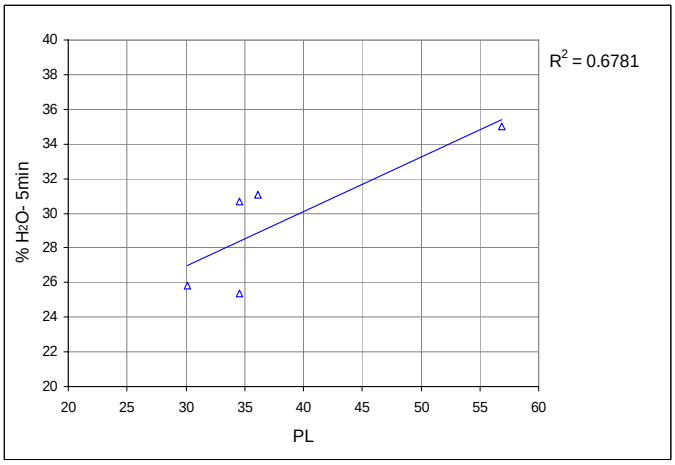

Figure 19 – Effect of PL on percent water content of accreted solids (t=5 min).

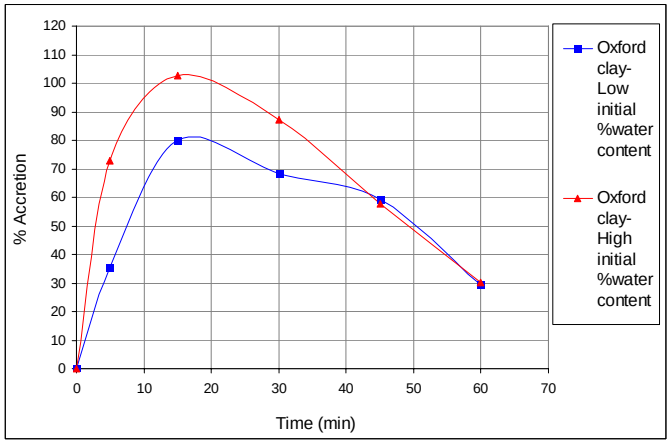

Figure 22 – Effect of initial water content on accretion-time profile.

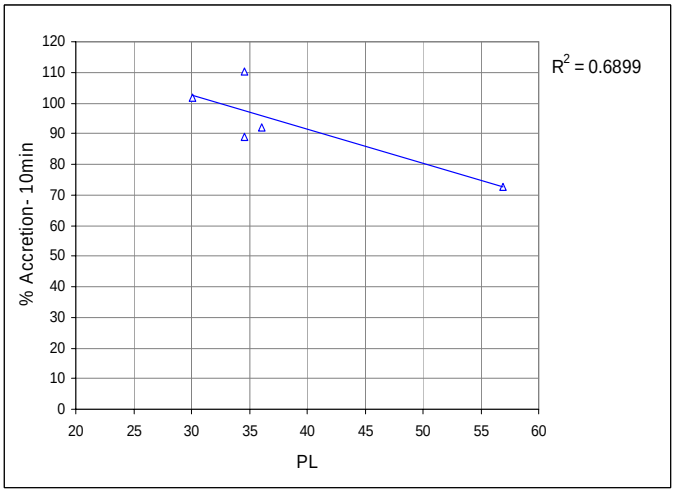

Figure 20 – Effect of PL on accretion (t=10 min).

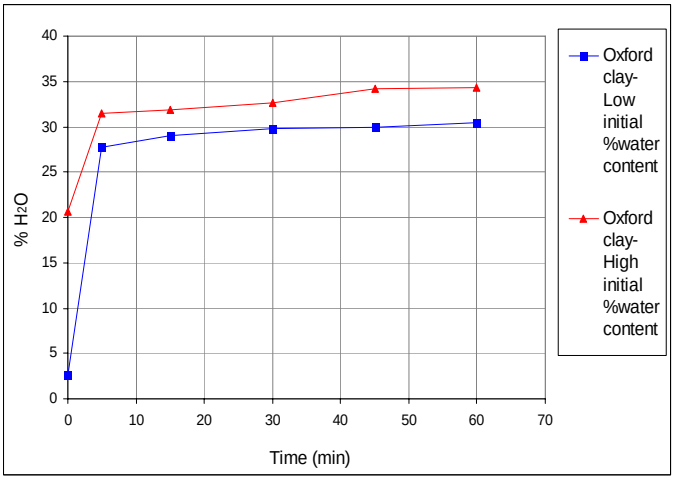

Figure 23 – Effect of initial water content on hydration of accreted solids vs. time.

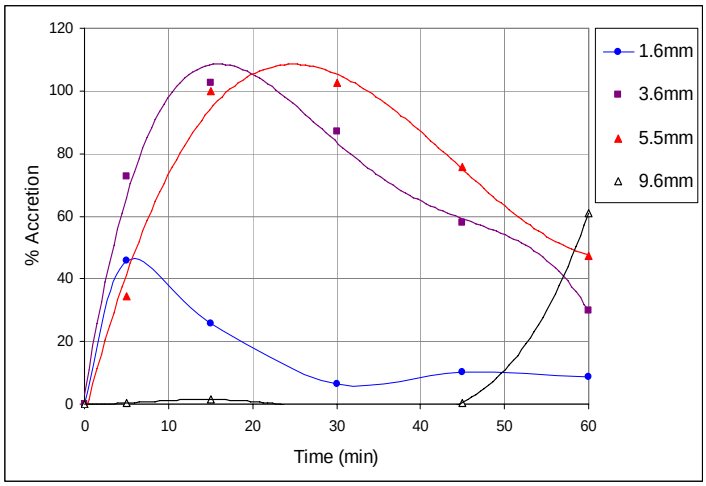

Figure 24 – Effect of cuttings size (Oxford clay) on accretion-time profile.

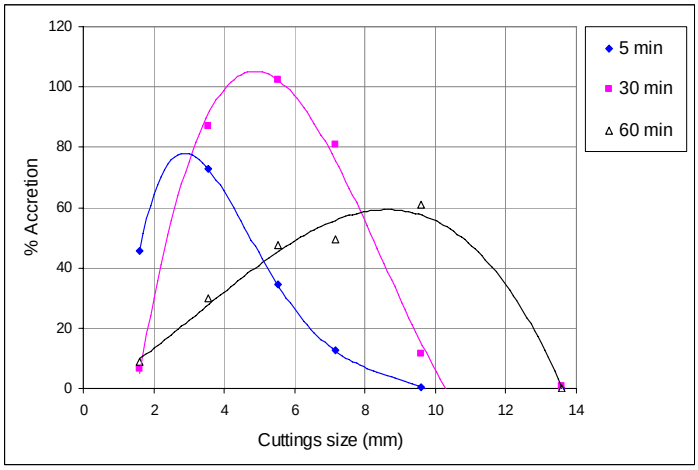

Figure 25 – Effect of cuttings size (Oxford Clay) on accretion maxima.

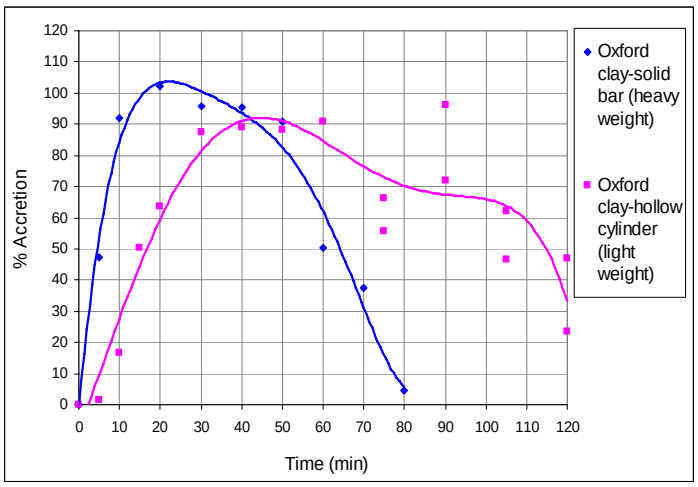

Figure 26 – Effect of bar weight on accretion of Oxford Clay.

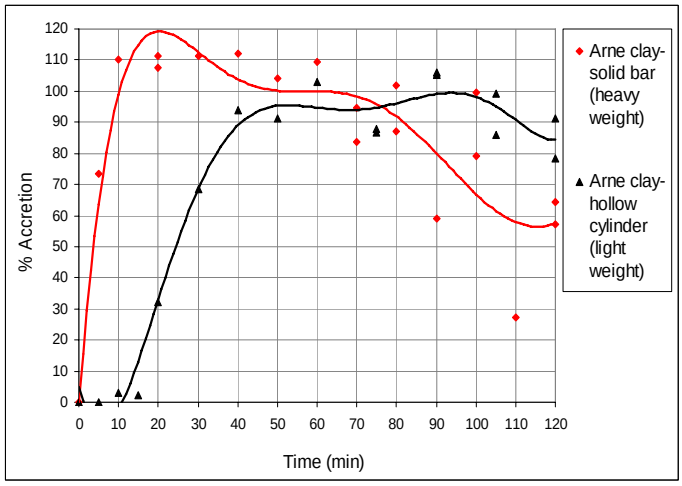

Figure 27 – Effect of bar weight on accretion of Arne Clay.

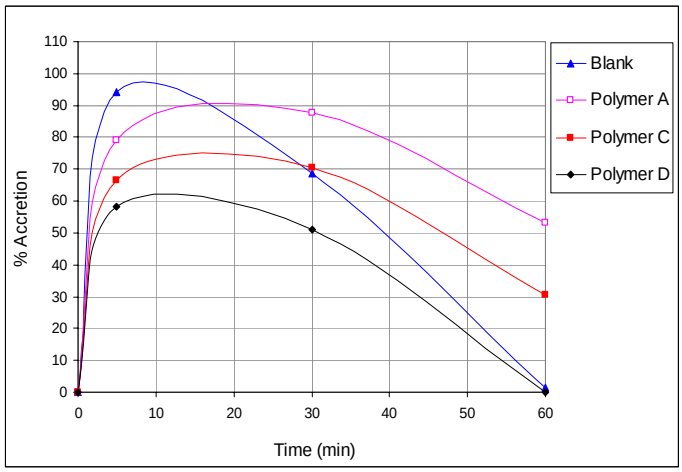

Figure 28 – Effect of encapsulating polymer on accretion-time profile.

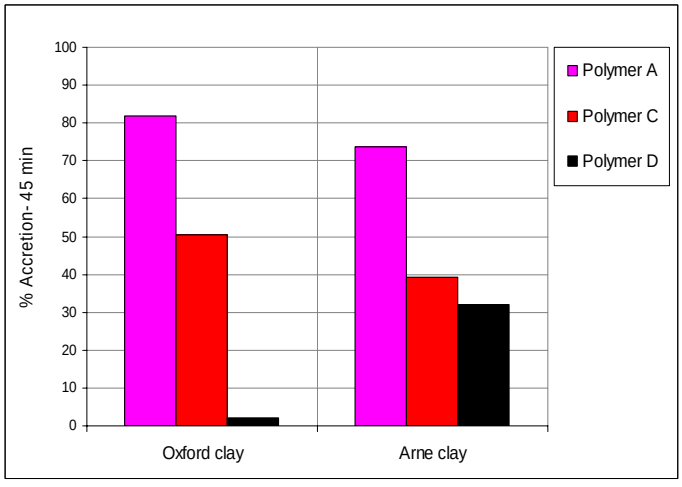

Figure 29 – Effect of encapsulating polymer on accretion (t=45 min).

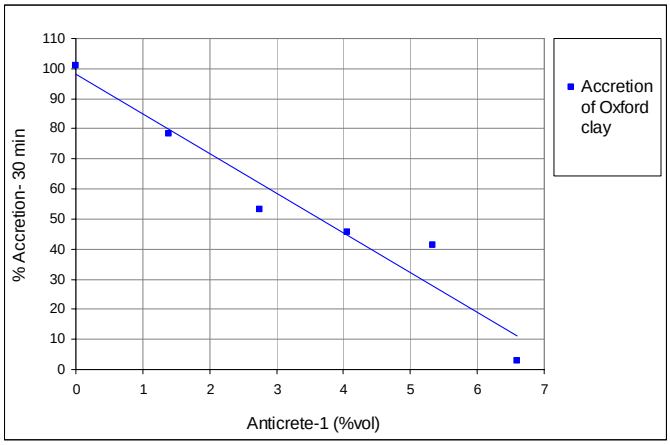

Figure 30 – Effect of anticrete concentration on accretion (t=30 min).

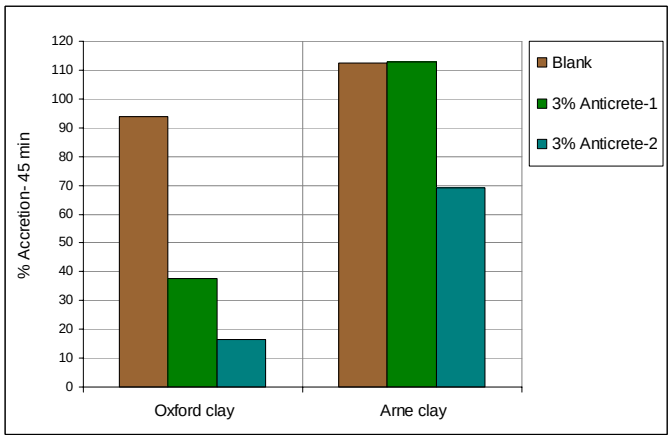

Figure 31 – Effect of variations in anticrete composition on accretion (t=45 min).

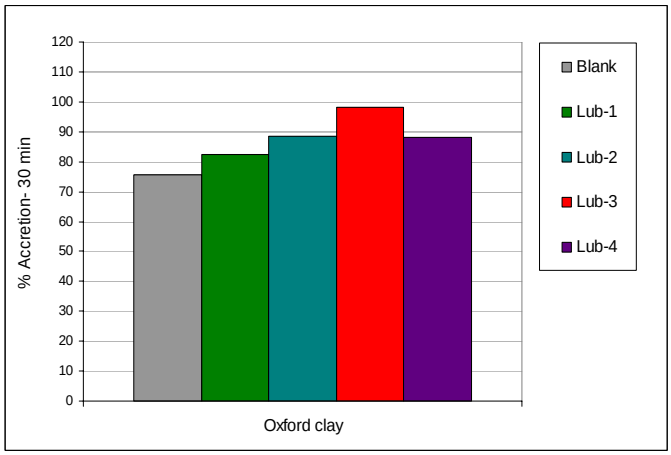

Figure 32 – Effect of lubricants on accretion (t=30 min).